Numerical Simulation of Phase Space Advection in Fusion Plasmas

M. R. Dorr, R. H. Cohen, M. A. Dorf and J. A. F. Hittinger
Lawrence Livermore National Laboratory

P. Colella and D. F. Martin
Lawrence Berkeley National Laboratory

SciDAC 2010 Meeting
July 13, 2010

LLNL-PRES-430096

This work performed under the auspices of the U.S. Department of Energy by Lawrence Livermore National Laboratory under Contract DE-AC52-07NA27344.

Research supported by the Office of Advanced Scientific Computing Research of the US Department of Energy under contract number DE-AC02-05CH11231.

Our motivating application is the simulation of fusion reactor edge plasmas

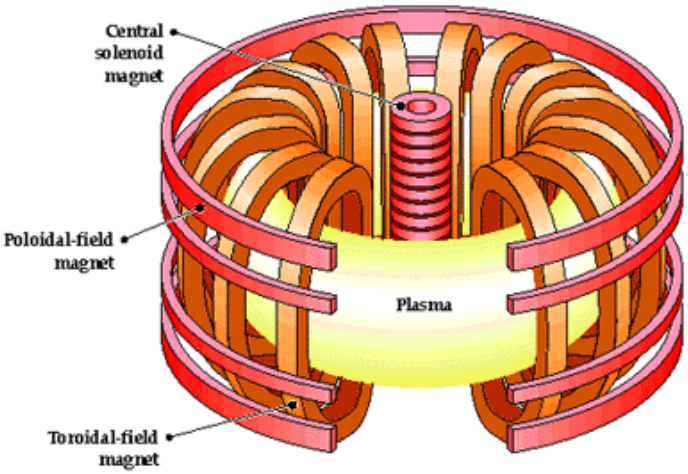

Simulation of edge plasma turbulence in tokamak fusion reactors requires kinetic models to describe phenomena such as the formation of the pedestal, a steep-gradient region that develops spontaneously in high-performance (H-mode) discharges.

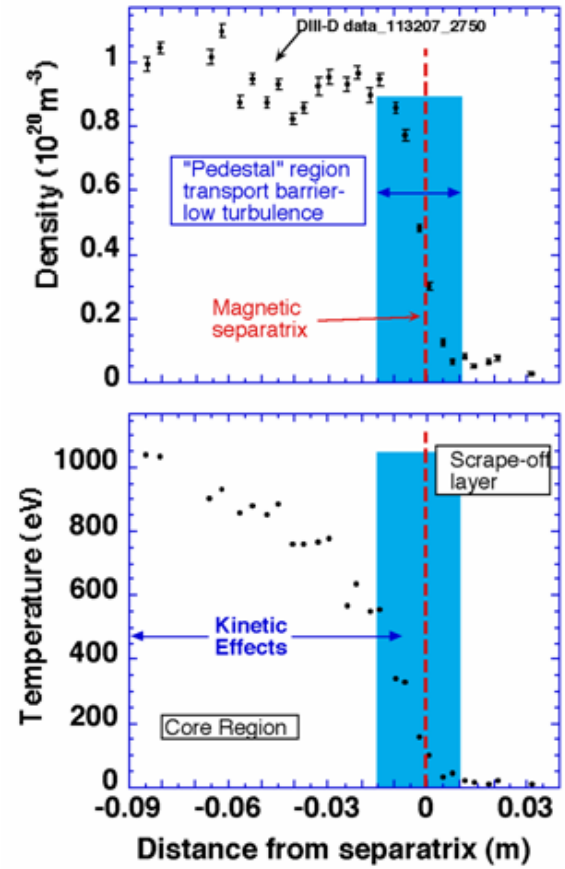

The edge pedestal density (ne) and temperature (Te) profiles near the edge of an H-mode discharge in the DIII-D tokamak. The horizontal scale is distance from nominal boundary of the plasma at R= 2.34m [from G.D. Porter, et al., Phys. Plasmas 7 (7), 3663 (Sept. 2000)].

Gyrokinetic models are well established in plasma physics, but raise new challenges for edge simulation

- Used to simulate core turbulence for many years
  - GS2 (Dorland, Kotschenreuther)
  - GENE (Jenko)
  - GYRO (Candy)
- Describes the evolution of distribution functions f(t,x,v) in (x,v) phase space, decoupling the gyromotion from the remaining dynamics
- Relies on the asymptotic development of a coordinate system in which distribution functions are symmetric with respect to gyrophase (which can then be ignored)
  - Reduces 6D phase space to 5D
  - Removes the gyrofrequency as a fast time scale
  - Validity of orderings in all regimes is still an open research question
  - Leads to more complicated field models
- Often assumes a "δf" formulation: $f = f_0 + \delta f$, where f_0 is a known Maxwellian distribution
  - Facilitates some linearization
  - Helps reduce noise in particle codes
  - *But, we don't know f_0 in the edge*

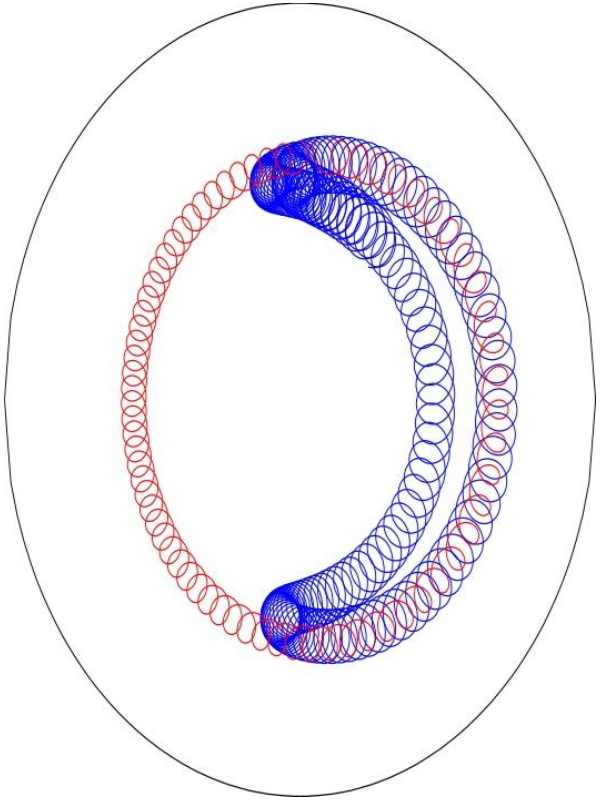

Source: http://iter.rma.ac.be

The gyrokinetic Vlasov equation describes the evolution of plasma species distribution functions

$$\frac{\partial B_{\parallel}^{*} f}{\partial t} + \dot{\mathbf{R}} \cdot \nabla_R (B_{\parallel}^{*} f) + \dot{v}_{\parallel} \frac{\partial}{\partial v_{\parallel}} (B_{\parallel}^{*} f) = 0$$

describes the evolution of a distribution function $f(\mathbf{R}, v_{\parallel}, \mu, t)$ in gyrocenter phase space coordinates, which in turn evolve as

$$\dot{\mathbf{R}} \equiv \frac{v_{\parallel}}{B_{\parallel}^{*}} \mathbf{B}^{*} + \frac{La}{ZB_{\parallel}^{*}} \mathbf{b} \times \mathbf{G}$$

$$\dot{v}_{\parallel} \equiv -\frac{1}{mB_{\parallel}^{*}} \mathbf{B}^{*} \cdot \mathbf{G}$$

where

$$\mathbf{B}^{*} \equiv \mathbf{B} + La \tfrac{m v_{\parallel}}{Z} \nabla_R \times \mathbf{b} \qquad B_{\parallel}^{*} = \mathbf{b} \cdot \mathbf{B}^{*}$$

$$\mathbf{G} \equiv Z \nabla_R \Phi + \frac{\mu}{2} \nabla_R B$$

$\mathbf{B}$ equilibrium magnetic field $\qquad B \equiv |\mathbf{B}|$

Φ equilibrium potential $\qquad \mathbf{b} \equiv \mathbf{B} / B$

La Larmor number (normalized gyroradius)

- The magnetic moment $\mu = m v_{\perp}^{2} / 2B$ is assumed a constant of the motion $(\dot{\mu} = 0)$
- Phase space volume is conserved

$$\nabla_R (B_{\parallel}^{*} \dot{\mathbf{R}}) + \frac{\partial}{\partial v_{\parallel}} (B_{\parallel}^{*} \dot{v}_{\parallel}) = 0$$

The gyrokinetic Vlasov equation is expressed in conservation form as:

$$\frac{\partial B_{\parallel}^{*} f}{\partial t} + \nabla_R (\dot{\mathbf{R}} B_{\parallel}^{*} f) + \frac{\partial}{\partial v_{\parallel}} (\dot{v}_{\parallel} B_{\parallel}^{*} f) = 0$$

Calculation of the charge density from gyrocenter dfns makes the Poisson solve more complicated

Poisson:

$$\varepsilon_0 \Delta\Phi(x) = e\left(n_e(x) - \sum_i Z_i n_i(x) \right)$$

x = lab frame coordinate

i = species index

The ion species number density is the sum of gyrophase-independent and gyrophase-dependent parts:

$$n_i(x) = \bar{n}_i(x) + \tilde{n}_i(x)$$

Gyroaveraged gyrocenter density:

$$\bar{n}_i(x) \equiv \frac{2\pi}{m_i} \int f_i(x, v_\parallel, \mu, t) B_\parallel^*(x, v_\parallel) dv_\parallel d\mu$$

Polarization density (long wavelength limit $(k_\perp \rho << 1)$

$$\tilde{n}_i(x) \equiv \frac{e}{m_i \Omega_i^2} \nabla_\perp \cdot (n_\alpha \nabla_\perp \Phi(x))$$

Gyrokinetic Poisson equation:

$$\nabla \cdot \left\{ \left[\varepsilon_0 \mathbf{I} + e^2 \sum_i \frac{Z_i \bar{n}_i}{m_i \Omega_i^2} (\mathbf{I} - \mathbf{b}\mathbf{b}^T) \right] \nabla\Phi \right\} = e\left(n_e - \sum_i Z_i \bar{n}_i \right)$$

Plasma edge geometries can be gridded using mapped multiblock coordinates

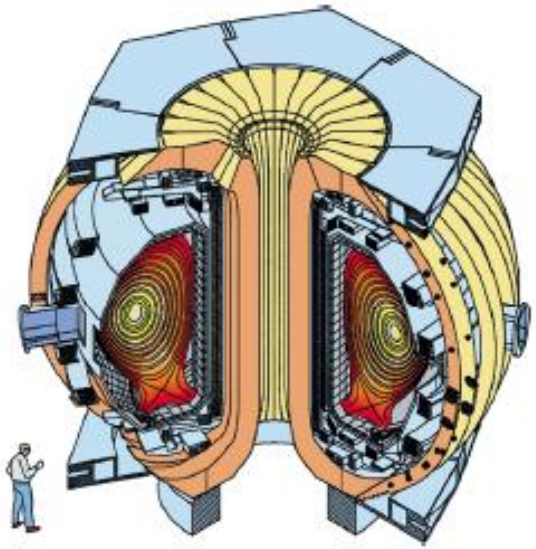

In 2D: A poloidal slice of the plasma edge is mapped to a multiblock, locally rectangular grid

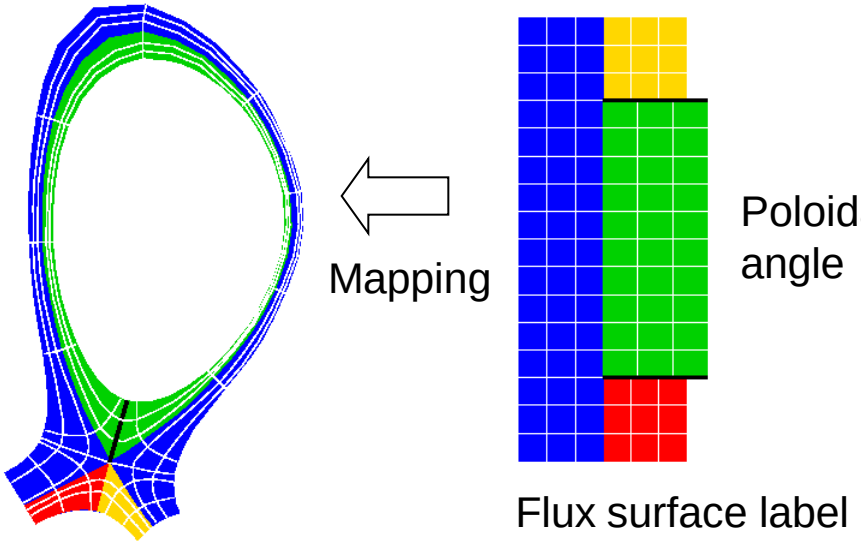

Physical coordinates

Computational coordinates

- The equilibrium magnetic field determines a mapping from physical to computational coordinates
- Alignment with flux surfaces facilitates treatment of strong anisotropies in discretization

In 3D: A toroidal component is added

Our finite volume discretization is based on a general, mapped grid formalism

Cartesian coordinates:

Spatial domain discretized as a union of rectangular control volumes

$$V_{\mathbf{i}} = [i_1 - \tfrac{h}{2}, i_1 + \tfrac{h}{2}] \times [i_2 - \tfrac{h}{2}, i_2 + \tfrac{h}{2}] \times \ldots \times [i_D - \tfrac{h}{2}, i_D + \tfrac{h}{2}]$$

Divergence theorem and coordinate change:

$$\int_{\mathbf{X}(V_i)} \nabla_{\mathbf{x}} \cdot \mathbf{F} d\mathbf{x} = \sum_{\pm=+,-} \sum_{d=1}^{D} \pm \int_{A_d^{\pm}} (\mathbf{N}^T \mathbf{F})_d \, d\mathbf{A}_{\xi}$$

where A_d are the high and low faces bounding V with normals pointing in the dth coordinate direction.

Mapped coordinates:

Smooth mapping from abstract Cartesian coordinates into physical space

$$\mathbf{X} = \mathbf{X}(\boldsymbol{\xi}), \quad \mathbf{X} : [0,1]^D \to \mathbf{R}^D$$

Then

$$\nabla_{\mathbf{X}} \cdot \mathbf{F} = \frac{1}{J} \nabla_{\xi} \cdot (\mathbf{N}^T \mathbf{F})$$

$$J = \det(\nabla_{\xi} \mathbf{X}), \quad (\mathbf{N}^T)_{p,q} \equiv \det[(\nabla_{\xi} \mathbf{X})(p \,|\, \mathbf{e}^q)]$$

where $A(p|v)$ denotes the matrix obtained by replacing the pth row of the matrix A by the vector v.

Fourth-order accurate flux divergence average is obtainable from fourth-order accurate cell face averages:

$$\boxed{\int_{\mathbf{X}(V_i)} \nabla_{\mathbf{x}} \cdot \mathbf{F} d\mathbf{x} = h^{D-1} \sum_{\pm=+,-} \sum_{d=1}^{D} \pm F^d_{\mathbf{i} \pm \frac{1}{2}\mathbf{e}^d} + O(h^4)}$$

where

$$\boxed{F^d_{\mathbf{i}+\frac{1}{2}\mathbf{e}^d} \equiv \sum_{s=1}^{D} \left\langle N_d^s \right\rangle_{\mathbf{i}+\frac{1}{2}\mathbf{e}^d} \left\langle F^s \right\rangle_{\mathbf{i}+\frac{1}{2}\mathbf{e}^d} + \frac{h^2}{12} \sum_{s=1}^{D} \left(\mathbf{G}_0^{\perp,d}\left(\left\langle N_d^s \right\rangle_{\mathbf{i}+\frac{1}{2}\mathbf{e}^d} \right) \right) \cdot \left(\mathbf{G}_0^{\perp,d}\left(\left\langle F^s \right\rangle_{\mathbf{i}+\frac{1}{2}\mathbf{e}^d} \right) \right)}$$

$\mathbf{G}_0^{\perp,d} =$ second-order accurate centered difference of $\nabla_{\xi} - \mathbf{e}^d \dfrac{\partial}{\partial \xi_d}$ and $\left\langle q \right\rangle_{\mathbf{i}+\frac{1}{2}\mathbf{e}^d} \equiv \dfrac{1}{h^{D-1}} \displaystyle\int_{A_d} q(\xi) d\mathbf{A}_{\xi} + O(h^4)$

Free-streaming is preserved in a natural way

For any smooth mapping $\boxed{\sum_{d=1}^{D} \frac{\partial N_d^s}{\partial \xi_d} = 0}$ where $\mathbf{N} = (N_d^s) = J\nabla_{\mathbf{x}}\boldsymbol{\xi}$ "Metric identities"

There exist functions $M_{d,d'}^s, d \neq d'$ such that $\boxed{N_d^s = \sum_{d \neq d'} \frac{\partial M_{d,d'}^s}{\partial \xi_{d'}}, M_{d,d'}^s = -M_{d',d}^s}$

$$N_d^s = -[\nabla_\xi \times (x_l \nabla_\xi x_m)]_d, \quad d = 1,2,3, \quad (d,l,m)\ cyclic$$

"Conservative form", Thomas and Lombard, AIAA J., 17(10), 1979.

$$N_d^s = [\nabla_\xi \times (x_m \nabla_\xi x_l)]_d, \quad d = 1,2,3, \quad (d,l,m)\ cyclic$$

Kopriva, J. Sci. Comput. 26(3), 2006

$$N_d^s = \tfrac{1}{2}[\nabla_\xi \times (x_m \nabla_\xi x_l - x_l \nabla_\xi x_m)]_d, \quad d = 1,2,3, \quad (d,l,m)\ cyclic$$

"Invariant form", Thomas and Neier, J. Spacecr. Rockets 27(2), 1990

Hence

$$\boxed{\int_{A_d} N_d^s d\mathbf{A}_\xi = \sum_{\pm=+,1} \sum_{d' \neq d} \pm \int_{E_{d,d'}^{\pm}} M_{d,d'}^s d\mathbf{E}_\xi}$$

where $E^{\pm}{}_{d,d'}$ are the (hyper)edges on the low and high sides of A_d in the d' direction.

COGENT (COntinuum Gyrokinetic Edge New Technology)

- Continuum GK equations in conservative form (T. S. Hahm, 1996)
- Geometry handled by flux surface aligned mapped multiblock grids
- 4th-order, finite-volume, mapped grid formalism
- Spatial discretization based on limited, centered fluxes
- RK4 time integrator
- Arbitrary number of plasma species
- PCG solver for long wavelength GK Poisson equation with kinetic electrons
- Boltzmann electron option
- Built on Chombo infrastructure (leveraging APDEC SciDAC effort):
  - Future development path to adaptive mesh refinement
  - Parallel in all phase space dimensions, with independent domain decomposition for configuration, velocity and phase space
  - Support for the 4th-order, finite-volume, mapped grid formalism

COGENT includes a Boltzmann electron option solved with a Newton-Krylov iteration

$$n_e = \frac{\left\langle \sum_i Z_i \bar{n}_i \right\rangle_j}{\left\langle \exp(\varphi / T_e) \right\rangle_j} \exp(\varphi / T_e)$$

Average over j-th flux surface

$$\langle u \rangle_j \equiv \sum_k w_{j,k} u(r_j, \theta_k)$$

GK Poisson-Boltzmann Newton Jacobian:

$$\mathbf{J} \equiv -\nabla \mathbf{N}^T \left(De^2 \mathbf{I} + \frac{La^2}{B^2} \sum_i m_i \bar{n}_i (\mathbf{I} - \mathbf{b}\mathbf{b}^T) \right) \mathbf{N} \nabla + \mathbf{diag}_j [\mathbf{N}_j(\varphi)(\mathbf{I} - \mathbf{e}^T \mathbf{w}_j \mathbf{D}_j(\varphi))]$$

Using the projection

$$\mathbf{P} \equiv \mathbf{diag}_j (\mathbf{e}\mathbf{w}_j^T)$$

solve the Jacobian system with BiCGStab with a two-phase preconditioner:

- P projected (tridiagonal solve)
- (I-P) projected (Hypre multigrid)

$$\mathbf{N}_j(\varphi) \equiv \frac{\left\langle \sum Z_i \bar{n}_i \right\rangle_j}{T_e} \mathbf{D}_j(\varphi)$$

$$\mathbf{e} \equiv (1, 1, \ldots, 1)$$

$$\mathbf{w}_j \equiv (w_{j,1}, w_{j,2}, \ldots, w_{j,N})$$

$$\mathbf{D}_j(\varphi) \equiv \left\langle \exp(\varphi / T_e) \right\rangle_j^{-1} \mathbf{diag}_{k=1}^{k\max} (\exp(\varphi_{j,k}) T_e)$$

A geodesic acoustic mode (GAM) is an eigenmode of the GK Vlasov-Poisson system in a torus

Ion acoustic waves exist even in collisionless plasmas:

$$\frac{\omega}{k} = v_s = \left(\frac{T_e + \gamma_i T_i}{m_i} \right)^{1/2}$$

Collisionless damping can occur depending upon v_s and the distribution function shape

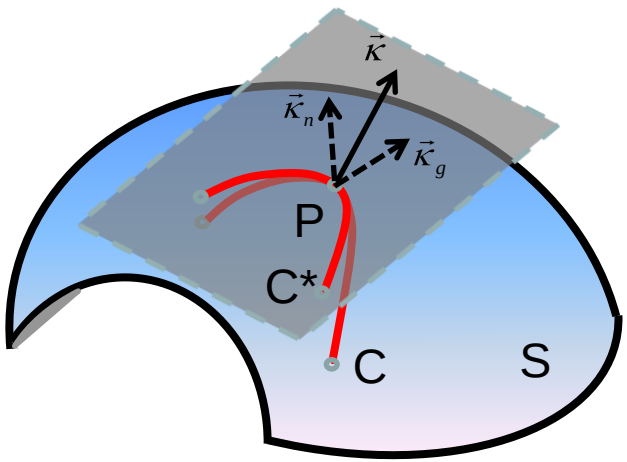

A GAM is a consequence of the components of the E X B force acting to keep particles on field lines, which is related to the geodesic curvature, which is related to the safety factor q.

Dispersion analyses yield frequencies and damping rates, e.g., for *q* large (Gao et al., Phys. Plasmas 15, 072511 (2008)):

$$\omega^2 = \left(\frac{7}{4} + \tau \right) \frac{v_{ti}^2}{R^2} \left[1 + \frac{46 + 32\tau + 8\tau^2}{(7+4\tau)^2 q^2} \right]$$

$$\gamma = -i \frac{\pi^{1/2}}{2} \frac{v_{ti}}{R} \frac{(R\omega / v_{ti})^6}{7/4 + \tau} q^5 \exp\left[-\left(\frac{qR\omega}{v_{ti}} \right)^2 \right]$$

where $v_{ti} = (T_i / m_i)^{1/2}$ $R =$ major radius

$\tau = T_e / T_i$ $q =$ safety factor

GAM density and potential in the Miller equilibrium geometry

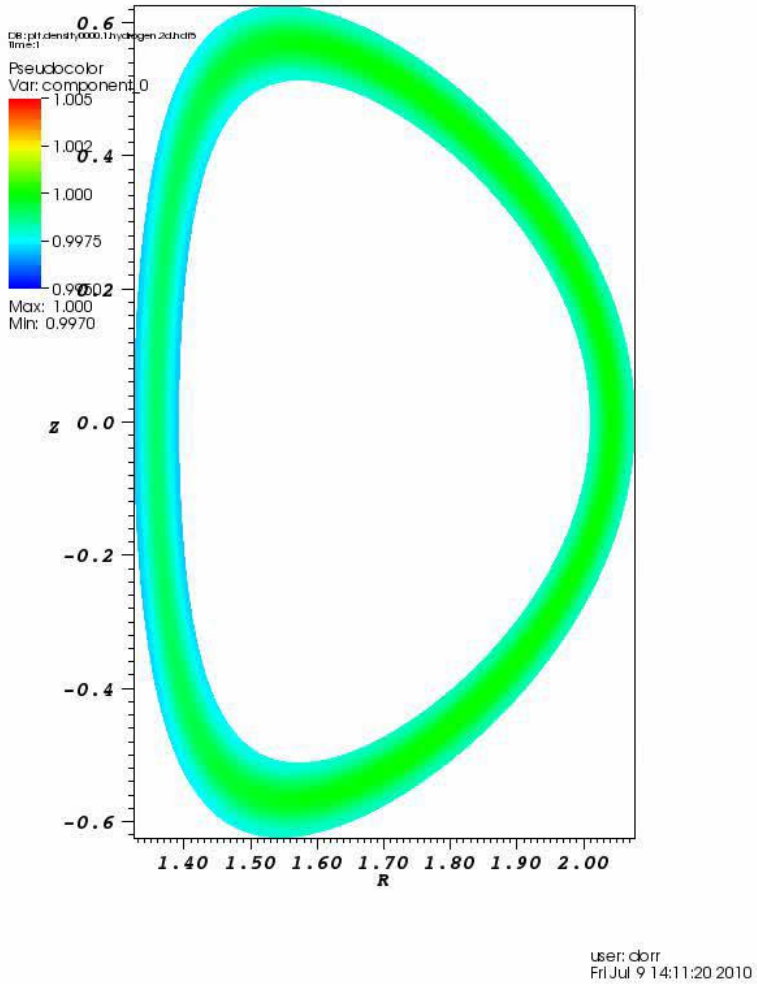

Density

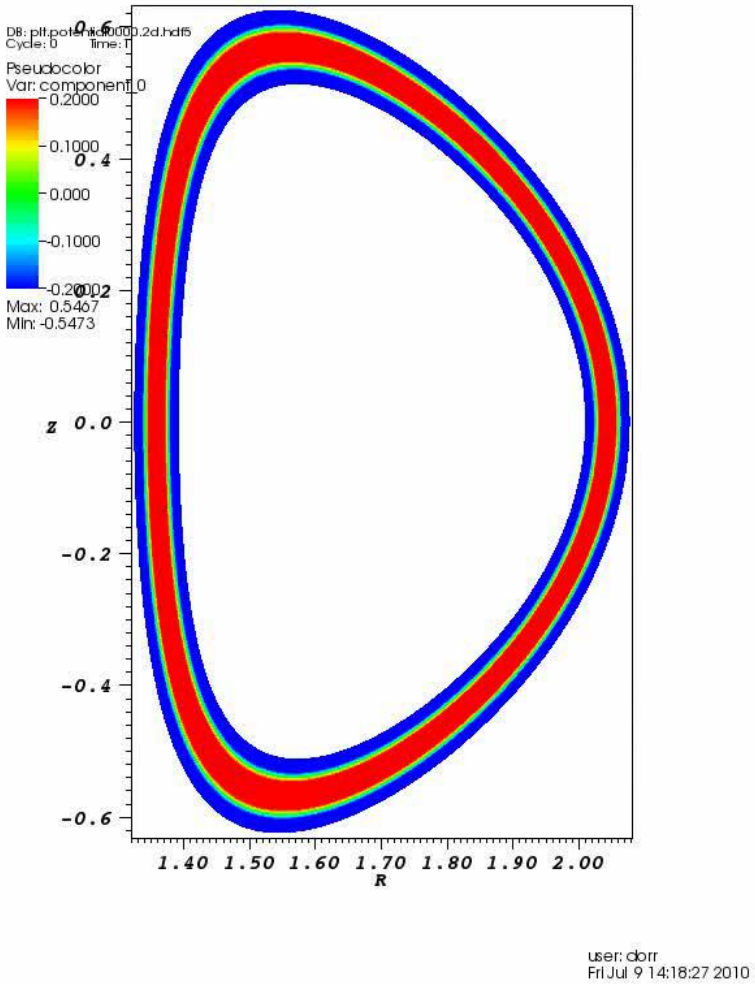

Potential

COGENT predictions of GAM frequencies and damping rates agree with analytic dispersion models

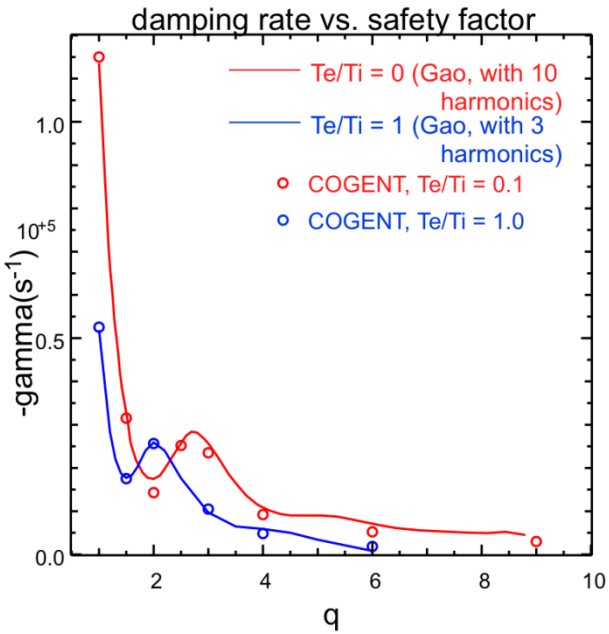

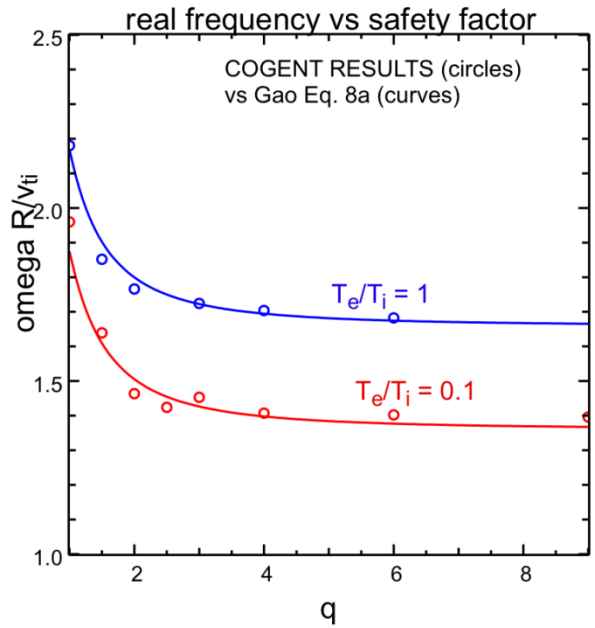

Potential at fixed probe at outboard midplane vs. time

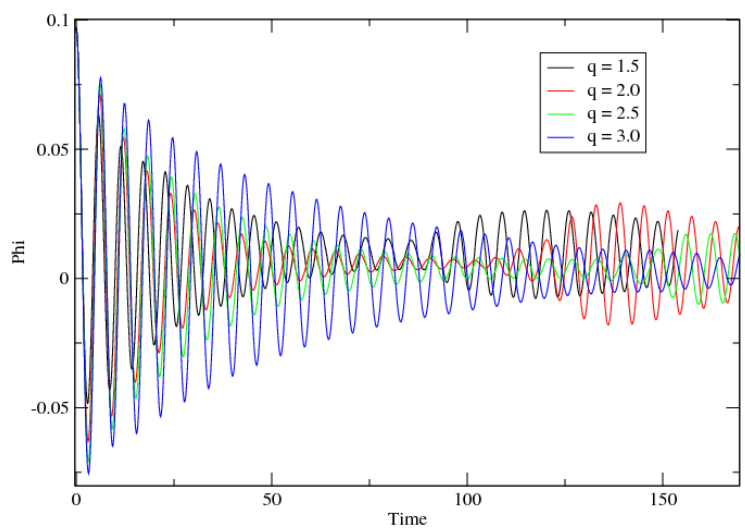

Comparison of GAM runs at varying phase space resolution verifies fourth-order convergence

Grid refinement level (N)	Grid (radial x poloidal x vparallel x mu)	Estimated density error conv. rate (r)	Richardson extrapolated density error (ε)
1	8 x 32 x 32 x 8		
2	16 x 64 x 64 x 16		
3	32 x 128 x 128 x 32	3.8 (L1) 3.8 (L2) 4.1 (Max)	3.37×10^{-7} (L1) 6.03×10^{-7} (L2) 1.95×10^{-4} (Max)
4	64 x 256 x 256 x 64	4.2 (L1) 4.1 (L2) 3.6 (Max)	1.40×10^{-8} (L1) 2.95×10^{-7} (L2) 1.69×10^{-5} (Max)

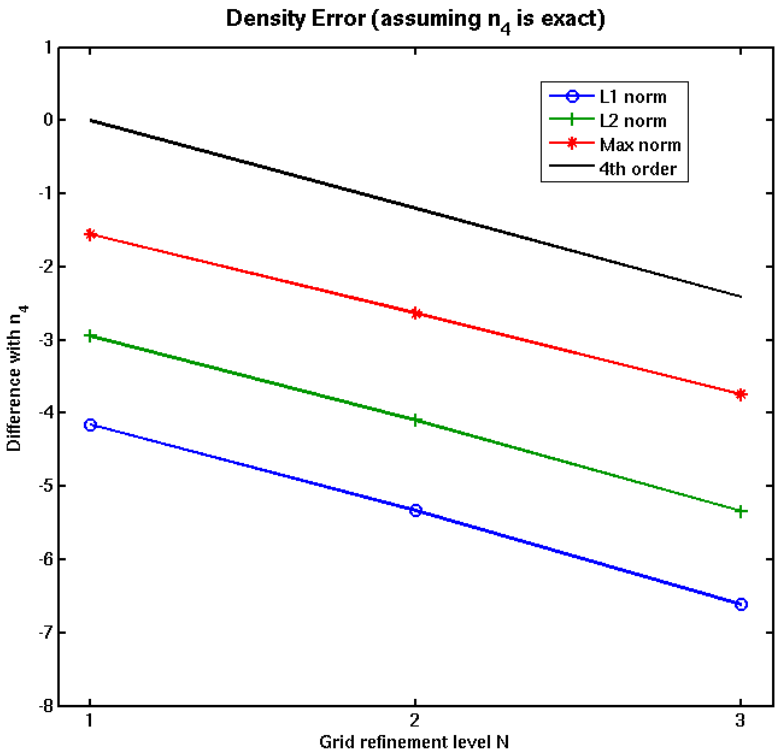

n_i = density at refinement level i

$d_i = \| n_{i+1} - n_i \|_x$, x = L1, L2, Max

Rate estimate: $r = \log(d_{i+1}/d_i) / \log(2)$

Error estimate: $\varepsilon = \log(d_i) / (1 + 2^r)$

Our algorithm development supports the Edge Simulation Laboratory (ESL) roadmap for a continuum edge plasma simulation capability

Nonlinear, full-f phase space advection model
- Multiblock diverted geometry
- Field line shear in 5D

Collision model
- Target operator TBD
- Mapped FV discretization applicable to Fokker-Planck-type operators

Algorithms with well understood and controllable (phase) spatial and temporal error

Multiresolution and multiscale algorithms
- IMEX
- AMR

Verified model implementation

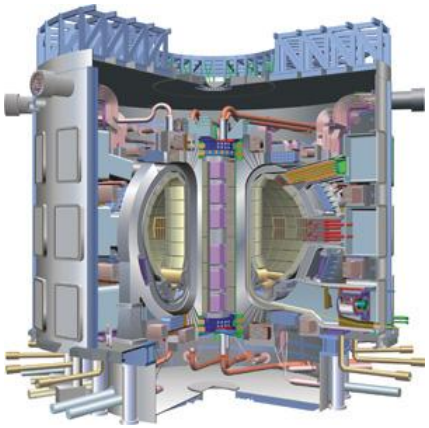

Gyrokinetic models

Exascale capabilities

Improved gyrokinetic models or ?

Codes validated with experiment